The inverse problem for simple classical liquids: a density functional approach

1997 J. Phys.: Condens. Matter 9 L89

(http://iopscience.iop.org/0953-8984/9/7/004)

J. Phys.: Condens. Matter **9** (1997) L89–L98. Printed in the UK PII: S0953-8984(97)79859-X

LETTER TO THE EDITOR

The inverse problem for simple classical liquids: a density functional approach

Yaakov Rosenfeld† and Gerhard Kahl‡

† Physics Department, Nuclear Research Centre Negev, PO Box 9001, Beer-Sheva 84190, Israel
‡ Institut fur Theoretische Physik, TU Wien, Wiedner Hauptstraße 8–10, A-1040 Wien, Austria

Received 27 November 1996

Abstract. A recently introduced algorithm for solving the inverse problem for simple classical fluids (i.e. the deduction of the interatomic interaction from structural data), which is based on the fundamental-measure free-energy density functional for hard spheres, is analysed in comparison with other methods. In a benchmark test for the Lennard-Jones system near the triple point, it is comparable with about *ten simulations* in the iterative predictor–corrector scheme proposed some years ago by Levesque, Weis, and Reatto. The method is used to extract the effective pair potential of Kr from very accurate experimental neutron scattering structure factor data.

The inverse problem, i.e. the deduction of the interatomic interaction from structural data obtained from scattering experiments, has been the object of much attention [1–15] in the physics of liquids. The determination of the interatomic interaction in condensed matter is of fundamental importance. Although many-body forces are always present in condensed systems, even in monatomic systems, an effective state-dependent two-body interaction (a pair potential, $\varphi(r)$) is still an important and useful quantity. The insensitivity in a dense fluid of the pair radial distribution function $g(r)$ to the exact shape of the pair potential $\varphi(r)$ plays a major role in the solution of the direct problem, i.e. $\varphi(r) \rightarrow g(r)$. As a result, the solution of the inverse problem, i.e. $g(r) \rightarrow \varphi(r)$, requires a highly accurate and *non-perturbative* theory for the fluid structure. A non-perturbative theory should be equally applicable to quite disparate potentials (e.g., the hard-sphere and Coulomb ones), and the quest for such a theory has led to many developments. The simulation of model fluids provides the testing ground for theoretical methods and has played a key role in addressing both the 'direct' and 'inverse' problems.

The first non-perturbative accurate theory of fluid structure, the modified hypernetted-chain (MHNC) theory, was based on the *ansatz* of universality of the bridge functions [16]. Using the bridge functions for hard spheres, it proved accurate for the 'direct' problem, and motivated several other integral equation approximations [17, 18]. It also led to the first successful results for the solution of the inverse problem [7]. Yet, these 'inverse' results were not accurate enough in certain density–temperature regions of the fluid, and for certain types of liquids. The predictor–corrector method of Levesque, Weis, and Reatto (LWR) [11, 12], which is based on the MHNC scheme and on simulations, overcomes these drawbacks (at least in the one-component case): it can be applied to any liquid and gives reliable results even near the triple point. Applications to realistic systems (e.g. liquid Ga [13]) demonstrated the power of this approach. One should bear in mind, however, that in the iterative predictor–corrector algorithm each 'corrector' step is represented by a full computer simulation for a fluid with a given 'predictor' pair potential, and about ten

0953-8984/97/070089+10$19.50

such iteration steps are required near the triple point. The initial guess is provided by the MHNC equation with the hard-sphere bridge functions. The convergence of the iterative predictor–corrector procedure is due to the general high accuracy of the approximation of universality of the bridge functions. The generalization of the predictor–corrector formalism to the binary case is straightforward, but its realization [14] is by no means trivial and even fails in some cases: for small concentrations of the minority component the statistical errors in the computer simulation ('corrector') steps accumulate and the simulation does not lead to satisfactory results.

A recent development in density functional theory is the fundamental-measure functional (FMF) for the free energy of hard spheres and hard convex bodies [19–24]. The FMF, which is based on geometrical rather than van-der-Waals-like considerations, brings together the Percus–Yevick [25] and scaled-particle [26] theories. It is the first free-energy functional for hard spheres with adequate properties of crossover between different effective dimensionalities of the fluid, which result from spatial confinement of the fluid by external potentials. Due to its accuracy, the FMF enabled the extension of the approximation of universality of the bridge *functions* to that of universality of the bridge *functional* [22]. This provides an accurate non-perturbative theory for the static structure of fluids [22, 15] which also enables one to overcome [15] the problems encountered by the predictor–corrector algorithm for the inverse problem for mixtures. As we recently demonstrated [15], the interaction potentials extracted from the simulation pair correlation data are accurate to such an extent that this method can become a more efficient alternative to the use of simulations in the inversion problem.

In this letter we highlight the special features of this method [22, 15] in comparison with other possible schemes for solving the inverse problem. We further test the density functional method by comparison with the LWR-simulation predictor–corrector results [11, 12] for the Lennard-Jones (LJ 12–6) system near the triple point. We find that the potential obtained by our method is comparable to that obtained by about *ten* simulation predictor–corrector steps. We apply this method to very accurate scattering experiments on Kr [27], and extract the effective pair potentials from the experimental structure factor data.

The exact diagrammatic MHNC equation has the following form:

$$\beta\varphi(r) + b(r) = g(r) - 1 - c(r) - \ln g(r) \tag{1}$$

where $c(r)$ is the usual Ornstein–Zernike direct correlation function given by

$$h(r) - c(r) = \rho_0 \int \mathrm{d}\boldsymbol{r}'\ c(|\boldsymbol{r} - \boldsymbol{r}'|)h(r') \tag{2}$$

where $h(r) = g(r) - 1$, ρ_0 is the bulk number density, and where hereafter we denote $1/k_BT$ as β. In terms of the Fourier transforms $\widetilde{h}(k)$ and $\widetilde{c}(k)$, and the structure factor $S(k)$, it reads

$$S(k) = 1 + \rho_0\widetilde{h}(k) = \frac{1}{1 - \rho_0\widetilde{c}(k)}. \tag{3}$$

When the bridge function is ignored, $b(r) = 0$, we have the hypernetted-chain (HNC) approximation

$$\varphi_{HNC}(r) = \frac{1}{\beta}(g(r) - 1 - c(r) - \ln g(r)). \tag{4}$$

Given a pair correlation function $g(r)$, the right-hand side of this equation is fully specified (with $c(r)$ given by the Ornstein–Zernike relation (2)), so we can regard it as a functional of $g(r)$:

$$\varphi_{HNC}(r) = \Phi_{HNC}[g(r)]. \tag{5}$$

We thus have the following exact relation:

$$\varphi(r) = \Phi_{HNC}[g(r)] - \frac{1}{\beta}b(r) \tag{6}$$

and the strategy for the solution of the inverse problem depends on how the information about the bridge function, $b(r)$, is given. Like in the diagrammatic analysis (see the discussion and the list of references in [16]), we consider the following two possibilities, (a) and (b).

(a) The bridge function is given as a *functional of the pair potential:*

$$b(r) = B[\varphi(r)]. \tag{7}$$

Within the diagrammatic analysis this case corresponds to (a1) the elementary diagrams with the Mayer f-bond [16]. It also corresponds to (a2) the simulation (indicated by the subscript sim) results for the structure with a *given* pair potential, for which we have

$$B[\varphi_{sim}(r)] = \beta\Phi_{HNC}[g_{sim}(r)] - \beta\varphi_{sim}(r). \tag{8}$$

When the bridge function is given as a functional of the pair potential (which is the quantity we seek!), then given the *experimental* pair structure *data* (or, if we just want to test the method, then given the simulation results for some test pair potential), $g_{data}(r)$, we are forced to use an iterative scheme (which is assumed to converge; see below):

$$\begin{aligned} &\varphi_0(r) = \Phi_{HNC}[g_{data}(r)] \\ &\varphi_{k+1}(r) = \varphi_k(r) + (\Phi_{HNC}[g_{data}(r)] - \Phi_{HNC}[g_k(r)]). \end{aligned} \tag{9}$$

These iteration cycles are based on the *approximation* of 'universality' (i.e. their insensitivity with respect to changes in the potential) of the bridge functions, in the form

$$\varphi_{k+1}(r) - \varphi_{data}(r) = -\frac{1}{\beta}(B[\varphi_k(r)] - B[\varphi_{data}(r)]). \tag{10}$$

But if and when they converge, $\varphi_\infty(r) = \varphi_{data}(r)$, the result is in principle exact if the functional $B[\varphi(r)]$ is exact. The converged result will, however, reflect approximations in the functional $B[\varphi(r)]$. In the LWR predictor–corrector scheme [11, 12] each iteration cycle in (9) is carried out as a full simulation run.

(b) The bridge function is given as a *functional of the pair correlation function:*

$$b(r) = B[g(r)]. \tag{11}$$

This case corresponds to (b1) the diagrammatic description of the bridge function in terms of a subset of the elementary diagrams (those with at least triply connected field points) with $g(r)-1$ bonds, to (b2) the MHNC approximation with a given ('universal') parametric set of bridge functions, and also to (b3) the density functional formalism.

When the bridge function is given as a functional of the pair correlation function there is no need for an iterative procedure: given the pair structure data, $g_{data}(r)$, we can immediately obtain the corresponding pair potential, via equation (6), from

$$\varphi_{data}(r) = \Phi_{HNC}[g_{data}(r)] - \frac{1}{\beta}B[g_{data}(r)] \tag{12}$$

where, of course, the inverted potential, $\varphi_{data}(r)$, will reflect approximations in the functional $B[g(r)]$.

The most important example of case (a) is the LWR predictor–corrector algorithm using simulations [11, 12]. The first important example of case (b) is the 'universality' approximation using the bridge functions for hard spheres of radius R [16, 9]:

$$b(r) = b^{HS}(r; R). \tag{13}$$

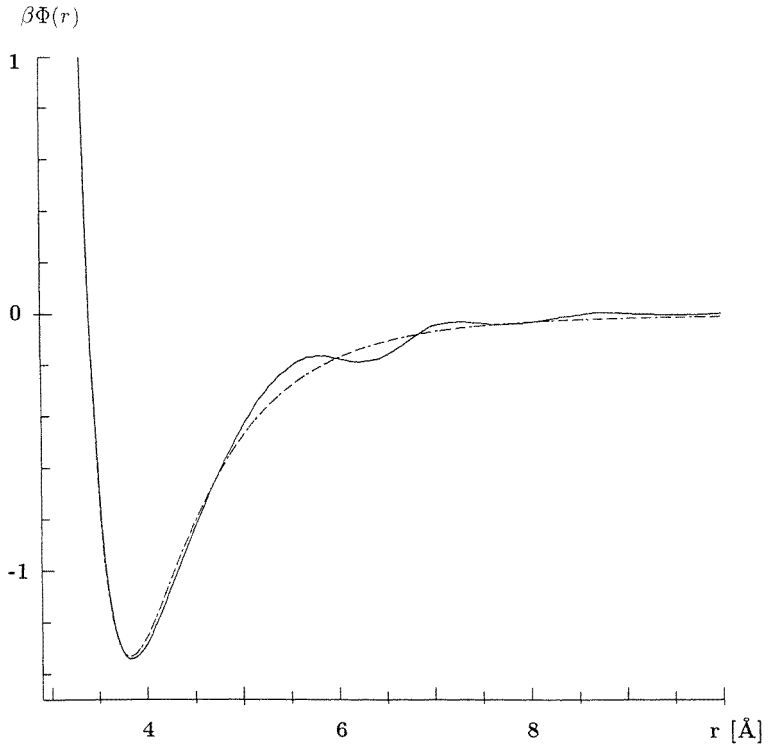

Figure 1. The inverted potential (full line) and original potential (Lennard-Jones, dot–dashed line) as functions of r for the Lennard-Jones system near the triple point, as specified in the text. The inverted potential was extracted from the 'experimental' $g(r)$ data, obtained in a molecular-dynamics simulation of 4096 particles over 20 000 time steps; the cut-off radius for the potential in the simulation was $6\sigma_{LJ}$.

Together with a condition for choosing the optimal (indicated by the subscript opt) $R = R_{opt}$, e.g. the extremum condition for the MHNC free energy [28],

$$\int \mathrm{d}^3 r \; [g_{data}(r) - g^{HS}(r)] \frac{\partial b^{HS}(r; R)}{\partial R} = 0 \qquad \text{for } R = R_{opt} \tag{14}$$

the relation (13) defines a functional dependence

$$B[g_{data}(r)] = b^{HS}(r; R_{opt}). \tag{15}$$

This allows one to obtain the MHNC inversion result

$$\varphi_{data}(r) \cong \varphi_{MHNC}(r) = \Phi_{HNC}[g_{data}(r)] - \frac{1}{\beta} b^{HS}(r; R_{opt}) \tag{16}$$

which provides a much better approximation than $\Phi_{HNC}[g_{data}(r)]$.

Indeed [11, 12], $\varphi_{MHNC}(r)$ was chosen as the starting point, i.e. the initial predictor, for the iterative predictor–corrector scheme. As a demonstration of the universality of the bridge functions [16], it is found [11, 12, 14] that $\varphi_{MHNC}(r)$ reproduces correctly the repulsive-core part of the interaction, and only in the vicinity of the triple point does one need many simulation predictor–corrector steps. The general validity of the universality of the bridge functions also implies the *monotonic* behaviour of the functional $B[\varphi(r)]$

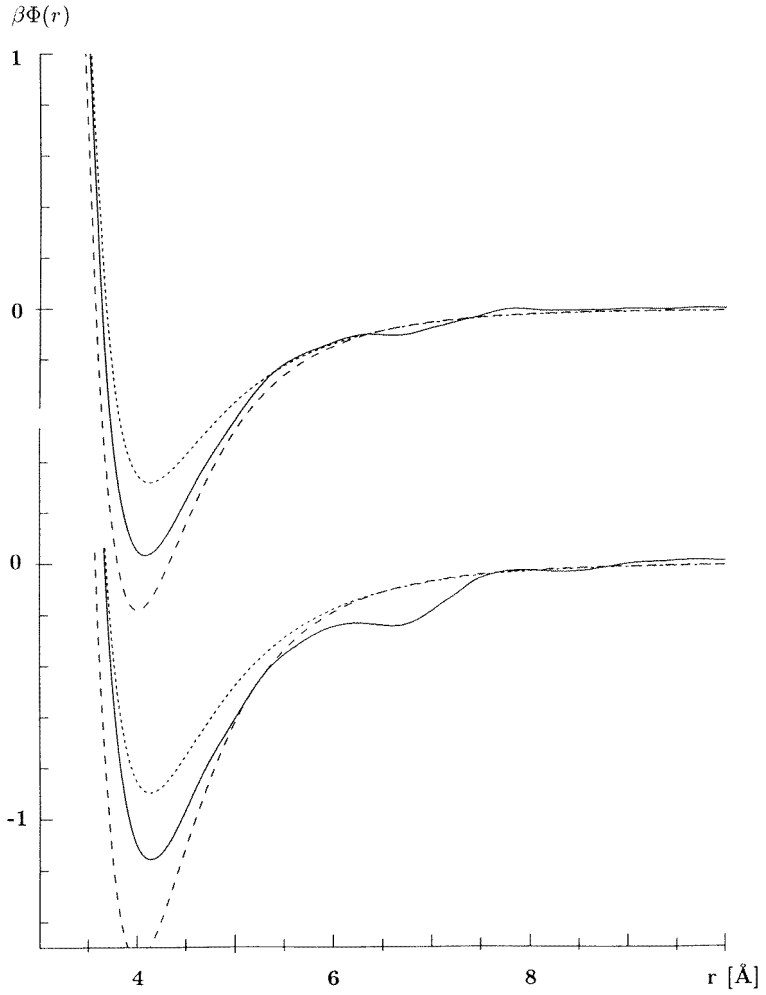

Figure 2. Inverted potentials (full lines) for two Kr states (as specified in the text) as functions of r from neutron scattering data [27]. The top curves correspond to $T = 169$ K, and the bottom curves to $T = 130$ K. In comparison we show a Lennard-Jones potential (dotted lines) with the usual parametrization for Kr (cf. [18]) and the Aziz–Slaman potential (broken line; cf. [33]).

in terms of the essential features of the the potential (notably the repulsive-core 'radius'), which is responsible for the convergence of the predictor–corrector scheme. In practice one can use in (13) and (14) either the parametrized simulation results for hard spheres [29] or the analytical solution of the Percus–Yevick equation [25], which give approximately the same results [9].

The central quantity in density functional theory (DFT) is the excess (over ideal-gas) free-energy functional, $F_{ex}[\rho(\boldsymbol{r})]$, of the density profile, $\rho(\boldsymbol{r})$. Taking the test-particle limit [30] for the bulk fluid with density ρ_0, $\rho(\boldsymbol{r}) = \rho_0 g(r)$, it is possible to obtain the bridge functional in the following form [22]:

$$B_{DFT}[g(r)] = \beta(-c^{(1,FD)}[\rho_0 g(r); r] - \mu_{ex}(\rho_0))$$

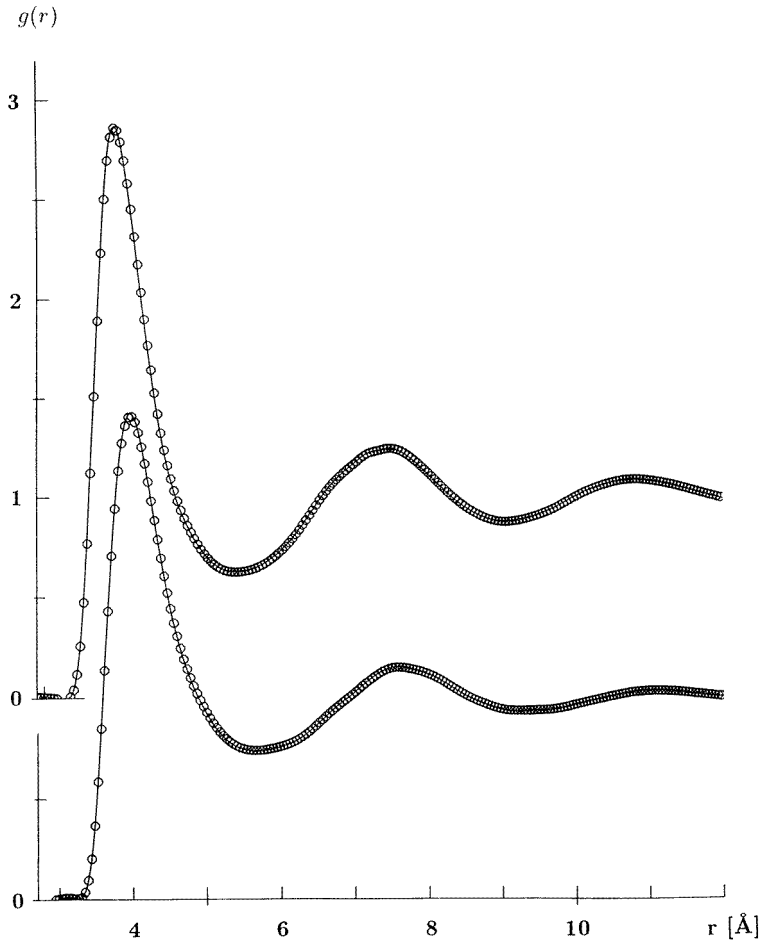

Figure 3. Pair distribution functions $g(r)$ as obtained from neutron structure factor data (symbols; [27]) for the two Kr states investigated in this letter: top—130 K and bottom—169 K. The full lines represent the theoretical integral equation results as obtained from the inverted potentials in figures 2 and 5.

$$+\rho_0 \int \mathrm{d}\boldsymbol{r}'\; c^{(2,FD)}[\rho_0;(|\boldsymbol{r}-\boldsymbol{r}'|)](g(r')-1) \tag{17}$$

where $\mu_{ex}(\rho_0)$ is the bulk excess chemical potential, and $c^{(n,FD)}$ are functional derivatives of the the excess free energy:

$$c^{(1,FD)}(\boldsymbol{r}) = -\beta\frac{\delta F_{ex}[\rho(\boldsymbol{r})]}{\delta\rho(\boldsymbol{r})} \qquad c^{(2,FD)}(\boldsymbol{r}_1,\boldsymbol{r}_2) = -\beta\frac{\delta^2 F_{ex}[\rho(\boldsymbol{r})]}{\delta\rho(\boldsymbol{r}_1)\,\delta\rho(\boldsymbol{r}_2)}. \tag{18}$$

However, the exact excess free-energy functional is generally not known, and we must resort to approximations. In particular, the FMF for hard-sphere mixtures [19–24] proved very accurate. With this functional it was possible to extend the approximation of universality of the bridge functions to that of 'universality of the bridge functional' [22]:

$$b(r) = B^{HS}_{DFT,FMF}[R;g(r)]. \tag{19}$$

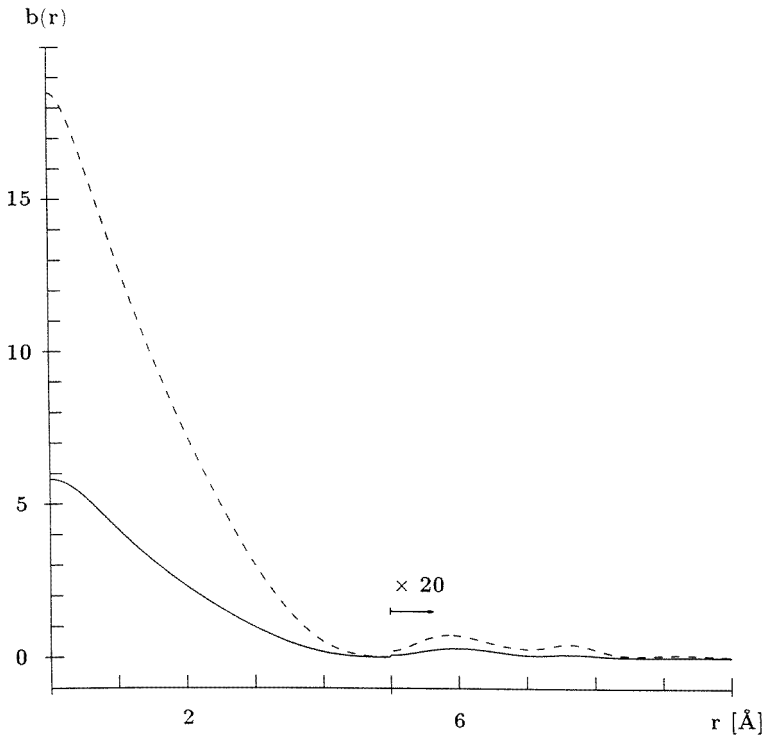

Figure 4. The bridge functions $b(r)$ as obtained from the experimental pair distribution functions (reference [27]) by using the FMF bridge functional for the two Kr states investigated in this letter; broken line: 130 K, with $2R_{opt} = 3.58$ Å (corresponding to $\eta = (4\pi/3)\rho R_{opt}^3 = 0.41$); full line: 169 K with $2R_{opt} = 3.47$ Å (corresponding to $\eta = 0.32$). Notice the change of scale (factor 20) for $r > 5$ Å.

The FMF bridge functional for the hard spheres, $B^{HS}_{DFT,FMF}[R; g(r)]$, depends parametrically on the hard-sphere radius R. The optimal value, $R = R_{opt}$, is obtained from the following equation [22]:

$$\int \mathrm{d}^3 r \; [g(r) - g^{HS}_{PY}(r)] \frac{\partial B^{HS}_{DFT,FMF}[R; g(r)]}{\partial R} = 0 \qquad \text{for } R = R_{opt} \tag{20}$$

which is similar to (14). Note, however, that in accordance with the build-up of the FMF functional we must use in (20) the Percus–Yevick (PY) equation [25] results for the hard-sphere pair function $g^{HS}_{PY}(r)$. By considering simulation data for given pair potentials we found that the resulting bridge functional

$$b(r) = B^{HS}_{DFT,FMF}[R_{opt}; g(r)] \tag{21}$$

is very accurate for both the direct and inverse problems, for both single-component fluids and mixtures [22, 15]. We would like to emphasize that the evaluation of $b_{data}(r) = B^{HS}_{DFT,FMF}[R_{opt}; g_{data}(r)]$ requires only several one-dimensional integrations. The inverted potentials obtained from more recent modifications [23] of the FMF functional are almost identical to those obtained from the original functional [22].

In practice $\Phi_{HNC}[g_{data}(r)]$ depends on the quality of the data and on the method for its handling. In particular, since both the simulation $g_{sim}(r)$ and the experimental structure

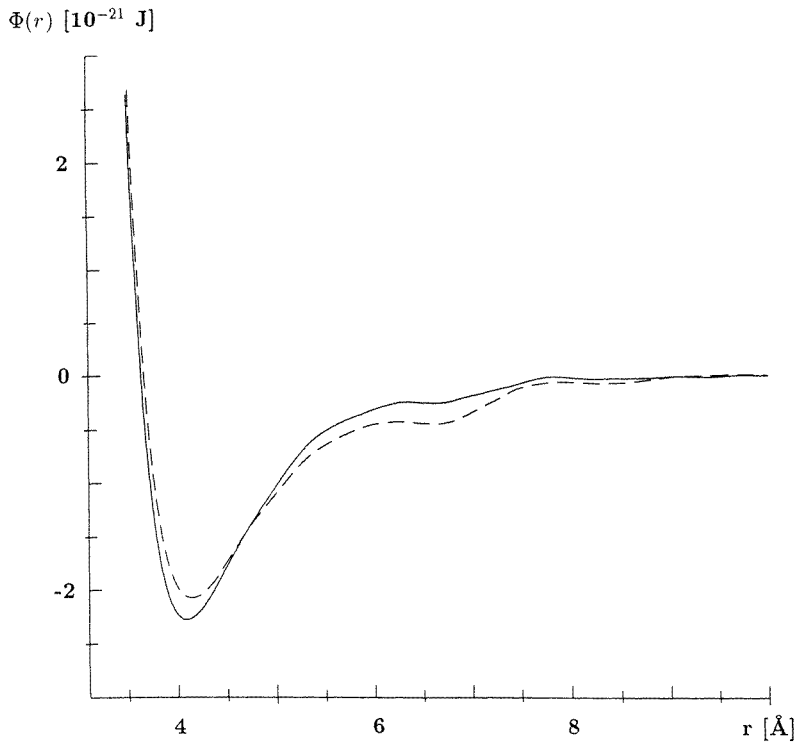

Figure 5. Inverted potentials for the two Kr states (as specified in the text) as functions of r from neutron scattering data [27], compared on a common scale. The full line corresponds to $T = 169$ K, and the broken like to $T = 130$ K.

factor $S_{data}(k)$, which is related to $g_{data}(r)$ by the Ornstein–Zernike equation, are given only over a limited range of their arguments (the distance r and the wave vector k, respectively), these data need to be 'extended' to cover the full range of r and k. There are several satisfactory schemes for solving this 'extension' problem (see, e.g., [31, 27, 32]). From the conceptual point of view (but, however, with little practical consequence), the extension method should be (and can be made to be) consistent with the inversion method.

Before applying our method to the recent high-quality set of experimental structure factor data for Kr [27], we would like to further gauge its accuracy against the benchmark which was used to test the LWR predictor–corrector algorithm [11, 12]. In figure 1 we compare the potential from our inversion method to the original LJ potential. The input structural data are the simulation results for the LJ system under triple-point conditions $\rho^\star = \rho\sigma^3 = 0.84$, $T^\star = k_B T/\varepsilon = 0.75$. This figure should be compared with figure 1 in [11], from which we find that the accuracy of our method is comparable with about ten iterations in the predictor–corrector procedure. In particular, this inversion yields a potential which is almost identical to the LJ potential, except for small wiggles after the minimum. We know from previous work [15] (and see figure 2 above) that these wiggles are much smaller when the first peak in $g(r)$ is smaller (i.e. at lower densities and/or higher temperatures). These wiggles reflect the imperfections of our bridge functional, which are demonstrably small. This means that if we begin with our result for the inversion problem

as the initial predictor potential in the LWR scheme, a single corrector simulation step (using this potential) will give us an estimate of the accuracy of our result and, at the same time, will provide a somewhat improved result (e.g. by smoothing and averaging the small wiggles after the minimum for the LJ potential). However, in view of the high accuracy of our inversion scheme, and the inherent statistical noise in the simulations, only little is expected to be gained from additional corrector steps by simulations.

In figure 2 we compare the potential from our inversion method with the LJ [18] and Aziz–Slaman [33] potentials for Kr at $T = 169$ K, $\rho_0 = 0.014\,57$ Å^{-3}, and $T = 130$ K, $\rho_0 = 0.017\,01$ Å^{-3}, respectively. These states correspond to $\rho^\star = 0.726, T^\star = 1.448$, and $\rho^\star = 0.848, T^\star = 1.114$, in reduced LJ units (recall [18] that $\varepsilon_{LJ} = 116.7$ K, $\sigma_{LJ} = 3.68$ Å). The input data are the experimental pair correlation functions, given in figure 3, which were obtained from very accurate neutron structure factor data for Kr [27]. The corresponding bridge functions, $b(r)$, are presented in figure 4. The apparently too high oscillations just after the first minimum (at about $r = 5$ Å) give rise to the wiggles in the inverted potentials. At shorter distances the bridge functions are accurate, while at larger distances they are too small to have an appreciable effect on the inverted potential. Finally, by comparing the inverted potentials at $T = 169$ K and $T = 130$ K on a common scale (figure 5) we find that they are very close, demonstrating the validity, in general, of the an effective state-independent pair potential for Kr. However, there are small but significant differences between the two potentials even near the minimum and at shorter distances. This indicates a weak density and temperature dependence of the effective pair potential for Kr, which can be accounted for [8, 27] by adding a three-body interaction to a state-independent pair potential. It will be interesting to repeat the analysis of the three-body interactions in view of the present, more accurate, effective two-body interactions.

In summary, we have demonstrated the high accuracy of our new algorithm for solving the inverse problem for simple classical fluids (i.e. the deduction of the interatomic interaction from structural data), which is based on the fundamental-measure free-energy density functional for hard spheres, and which can be easily applied to scattering results of real liquids even near the triple point.

The authors thank L Reatto (Milano) for interesting discussions, and R Magli (Firenze) for providing unpublished data. YR thanks Bob Evans (Bristol) and Jean-Pierre Hansen (Lyon) for interesting discussions and warm hospitality. This work was supported by the Benjamin Meaker Foundation, the French Ministry of Education, and by the Osterreichische Forschungsfonds Project No P11194.

References

[1] Johnson M D, Hutchinson P and March N H 1964 *Proc. R. Soc.* A **282** 283
[2] Gehlen P C and Enderby J E 1969 *J. Chem. Phys.* **51** 547
[3] Howells W S and Enderby J E 1972 *J. Phys. C: Solid State Phys.* **5** 1277
[4] Ailawadi N K, Banerjee P K and Choudry A 1974 *J. Chem. Phys.* **60** 2571
[5] Brennan M, Hutchinson P, Sangster M J L and Schofield P 1974 *J. Phys. C: Solid State Phys.* **7** L411
[6] Schommers W 1983 *Phys. Rev.* A **28** 3599
[7] Dharma-wardana M W C and Aers G C 1983 *Phys. Rev.* B **28** 1701
[8] Aers G C and Dharma-wardana M W C 1984 *Phys. Rev.* A **29** 2734
[9] Rosenfeld Y 1984 *Phys. Rev.* A **29** 2877
Rosenfeld Y 1986 *J. Stat. Phys.* **42** 437
[10] Dzugutov M, Larsson K-E and Ebbsjö I 1988 *Phys. Rev.* A **38** 3609
[11] Levesque D, Weis J-J and Reatto L 1985 *Phys. Rev. Lett.* **54** 451
Dharma-wardana M W C and Aers G C 1986 *Phys. Rev. Lett.* **56** 1211

Levesque D, Weis J-J and Reatto L 1986 *Phys. Rev. Lett.* **56** 1212
[12] Reatto L, Levesque D and Weis J-J 1986 *Phys. Rev.* A **33** 3451
[13] Bellisent-Funel M C, Chieux P, Levesque D and Weis J-J 1989 *Phys. Rev.* A **39** 6310
[14] Kahl G and Kristufek M 1994 *Phys. Rev.* E **49** R3568
[15] Kahl G, Bildstein B and Rosenfeld Y 1996 *Phys. Rev.* E **54** 5391
[16] Rosenfeld Y and Ashcroft N W 1979 *Phys. Rev.* A **20** 1208
Rosenfeld Y and Ashcroft N W 1979 *Phys. Lett.* **73A** 71
Rosenfeld Y 1980 *J. Physique Coll. Suppl.* **41** C2 77
[17] Talbot J, Lebowitz J L, Waisman E M, Levesque D and Weis J-J 1986 *J. Chem. Phys.* **85** 2187
[18] Hansen J-P and McDonald I R 1986 *Theory of Simple Liquids* 2nd edn (New York: Academic)
[19] See the reviews
Rosenfeld Y 1996 *Chemical Applications of Density-Functional Theory (ACS Symposium Series 629)* ed B Laird, T Ziegler and R Ross (Washington, DC: ACS)
Rosenfeld Y 1996 *J. Phys.: Condens. Matter* **8** 9287
[20] Rosenfeld Y 1989 *Phys. Rev. Lett.* **63** 980
Rosenfeld Y 1990 *J. Chem. Phys.* **93** 4305
Rosenfeld Y 1990 *Phys. Rev.* A **42** 5978
Rosenfeld Y, Levesque D and Weis J-J 1990 *J. Chem. Phys.* **92** 6818
[21] Rosenfeld Y 1994 *Phys. Rev.* E **50** R3318
Rosenfeld Y 1995 *Mol. Phys.* **86** 637
[22] Rosenfeld Y 1994 *Phys. Rev. Lett.* **72** 3831
Rosenfeld Y 1995 *J. Phys. Chem.* **99** 2857
Rosenfeld Y 1996 *Phys. Rev.* E **54** 2827
[23] Rosenfeld Y, Schmidt M, Lowen H and Tarazona P 1996 *J. Phys.: Condens. Matter* **8** L577
Rosenfeld Y, Schmidt M, Lowen H and Tarazona P 1997 *Phys. Rev.* E at press
[24] Rosenfeld Y 1996 *J. Phys.: Condens. Matter* **8** L795
[25] Percus J K and Yevick G J 1958 *Phys. Rev.* **110** 1
Wertheim M S 1963 *Phys. Rev. Lett.* **10** 321
Lebowitz J L 1964 *Phys. Rev.* A **133** 895
Lebowitz J L and Rowlinson J S 1964 *J. Chem. Phys.* **41** 133
[26] Reiss H, Frisch H and Lebowitz J L 1959 *J. Chem. Phys.* **31** 369
Reiss H 1992 *J. Phys. Chem.* **96** 4736
[27] Barocchi F, Chieux P, Magli R, Reatto L and Tau M 1993 *Phys. Rev. Lett.* **70** 947
Barocchi F, Chieux P, Magli R, Reatto L and Tau M 1993 *J. Phys.: Condens. Matter* **5** 4299
[28] Lado F 1982 *Phys. Lett.* **89A** 196
Lado F, Foiles S M and Ashcroft N W 1983 *Phys. Rev.* A **28** 2374
[29] Verlet L and Weis J-J 1972 *Phys. Rev.* A **5** 939
[30] Percus J K 1962 *Phys. Rev. Lett.* **8** 462
Percus J K 1964 *The Equilibrium Theory of Classical Fluids* ed H L Frisch and J L Lebowitz (New York: Benjamin) p II-33
[31] Foiles S M, Ashcroft N W and Reatto L 1984 *J. Chem. Phys.* **81** 6140
[32] Kambayashi S and Chihara J 1994 *Phys. Rev.* E **50** 1317
[33] Aziz R A and Slaman M J 1986 *Mol. Phys.* **58** 679